

Ringlike emission profiles in scanning near-field photoluminescence images of single InGaAs quantum dots

M. Geller,* I. Manke, K. Hodeck, R. Heitz, and M. Dähne

Institut für Festkörperphysik, Technische Universität Berlin, Hardenbergstraße 36, D-10623 Berlin, Germany

(Received 12 June 2001; published 27 November 2001)

In scanning near-field photoluminescence images of single InGaAs quantum dots taken with uncoated fiber tips, we observed sharp ringlike features varying in diameter with detection energy. This is in contrast to the typical single emission peaks observed using metal-coated fiber tips. These features can be explained by electrical charges induced by the uncoated fiber tip that lead to a Stark shift of the transition energy depending on the tip position. Simulations of the electric field at the quantum dot agree nicely with the experimental observation.

DOI: 10.1103/PhysRevB.64.233312

PACS number(s): 78.55.Cr, 07.79.Fc, 78.66.Fd

In conventional photoluminescence (PL) studies on semiconductor nanostructures using scanning near-field optical microscopy (SNOM),¹ metal-coated fiber tips are used in order to suppress the background from vicinal nanostructures.^{2,3} The background can also be reduced by performing SNOM PL experiments in internal-reflection geometry, i.e., by illumination and detection through the fiber tip.^{4–6} In this way, even uncoated fiber tips enable a remarkable spatial resolution and an appreciable background reduction.^{7,8}

Here we demonstrate that additional effects may contribute in experiments with uncoated fiber tips. When spatially imaging the PL signal at a constant detection energy, in most cases the emission profiles are characterized by very sharp ringlike structures instead of the expected single peak. Moreover, the diameters of the rings are found to vary strongly with detection energy. These observations can be explained by assuming a Stark shift of the transition energy in the quantum dot, which is due to an electric charge induced by the uncoated tip. In a detailed simulation of the electric field at the quantum dot as a function of the tip position, an excellent agreement with the experimental data is achieved.

The SNOM experiments were performed at room temperature using a homebuilt setup in internal-reflection geometry with fiber tips prepared by chemical etching.^{5–8} The $\text{In}_{0.4}\text{Ga}_{0.6}\text{As}$ quantum dots in a GaAs matrix were grown using metal-organic chemical vapor deposition (MOCVD).^{5,9,10} In a previous SNOM work at these quantum dots, Lorentzian linewidths of 10–20 meV were observed in the PL spectra at room temperature, considerably narrowing with decreasing temperatures.^{5,6} Mainly three peaks were observed, with typical transition energies at room temperature around 0.94 eV for the ground-state transition and 1.01 and 1.11 eV for the first and second excited-state transitions, respectively.

Figure 1(a) shows a PL image taken with a metal-coated fiber tip at a detection energy of 0.938 eV, displaying the emission from two quantum dots. Clearly evident from the cross section in Fig. 1(c) is an almost Gaussian shape of the signals from each dot. A corresponding PL image taken with an uncoated fiber tip is shown in Fig. 1(b). Now the spatial variation of the PL signal above the quantum dots is not

Gaussian anymore, but has a ringlike structure with diameters of about 250 nm and very sharp edges.

In order to analyze this astonishing effect in more detail, we studied the energy dependence. Representative results are shown in Fig. 2, where a single quantum dot is imaged at different detection energies, again using an uncoated fiber tip. It is clearly evident from the images that the shape and in particular the diameter of the ringlike emission features strongly vary with energy.

At a detection energy of 0.924 eV, the PL signal is reduced within a circle with a diameter of about 130 nm, marking the dot position. At 0.938 eV, where we would expect the ground-state transition, the intensity at the edges of the circle

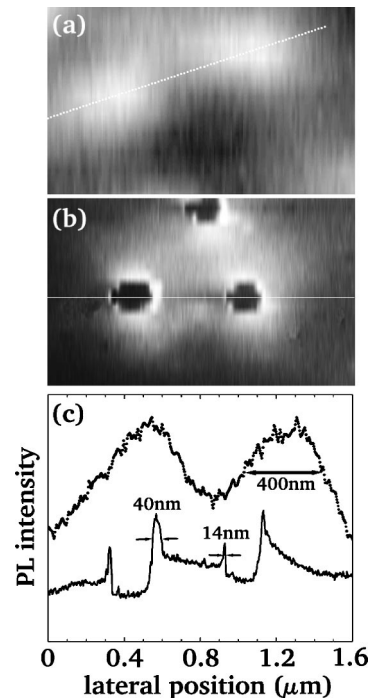


FIG. 1. PL image of InGaAs quantum dots taken at room temperature at a detection energy of 0.938 eV (a) with a metal-coated fiber tip and (b) with an uncoated fiber tip. (c) Intensity-contour plots along the lines in (a) and (b).

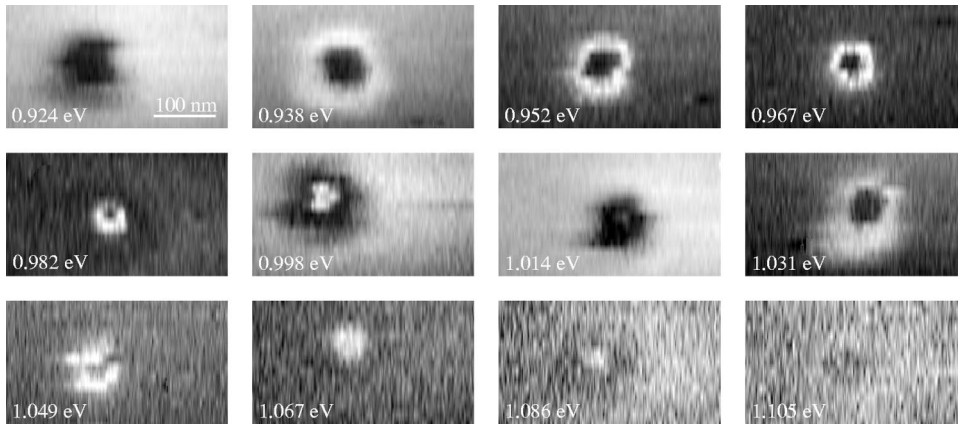


FIG. 2. PL images of a single InGaAs quantum dot taken with an uncoated fiber tip at room temperature for varying detection energies, showing the energy dependence of the ringlike features.

begins to increase, yielding a ringlike emission profile. Gradually this ring becomes sharper and its diameter decreases when further increasing the detection energy. At 0.998 eV the ring concentrates to an about 40 nm wide emission peak, while the signal intensity decreases around the peak. This peak disappears at 1.014 eV, which is about the energy of the first excited-state transition, and an emission profile is observed similar to the one for 0.924 eV. With further increasing detection energy, the signal profile changes again in a similar way as before, first forming a ring at 1.031 eV, which gradually decreases in diameter towards a peak at 1.067 eV that finally vanishes at detection energies between 1.086 and 1.105 eV.

In the following, the strong changes in emission characteristics when going from metal-coated to uncoated fiber tips are discussed. Only considering the results presented in Fig. 1(b), it could be assumed that a polarization effect of the tip is responsible for the ringlike emission features, as discussed in several SNOM studies.^{11–14} In the present case, the polarization would be related to the tip shape as well as to the structural properties of the quantum dot, which do not vary in size during the experiment. Therefore the strong variations in ring diameter with detection energy shown in Fig. 2 cannot be explained on the basis of polarization effects.

On the other hand, also a charging of the tip can occur when omitting its metal coating, resulting in an electric field in the vicinity of the tip. In several studies the influence of an electric field on the optical transitions in quantum dots was studied, leading to a Stark shift of the transition energies to lower values by several 10 meV,^{15–22} which is in the order of the energy changes where the variations in ring diameter are observed here.

In Fig. 3(a) we show schematically the charged tip above the dot. Based on structural data from MOCVD-grown dots, the dot shape comes close to a truncated pyramid.²³ In particular, transmission-electron microscopy images of the dots studied here yield a height of about 3 nm and a base length of about 17 nm, with the dot located about 30 nm underneath the surface.^{9,10} The low aspect ratio indicates that the dots are mainly polarizable in plane, yielding a much larger Stark shift by electric-field components in the x - y direction than by those in the z direction.

In this way, the observed ringlike structures can qualitatively be explained, as shown schematically in Fig. 3: The

electric-field component in the x - y direction is zero directly above the dot, increasing to a maximum at a certain lateral distance and then decreasing again. The corresponding Stark effect leads to a redshift with increasing electric field, resulting in an energy variation as shown in Fig. 3(b). Thus the transition energy in the dot is tuned to the detection energy at four different lateral positions along the cross-sectional line, which would in principle result in two concentric ringlike emission features. Since the collection efficiency of the tip decreases strongly at larger lateral distances, as shown in Fig. 3(c), the signal from the outer ring will be too weak to be detectable, so that only the inner ring remains visible. Now the diameter of this ring decreases with increasing detection energy, as observed in Fig. 2. The strong energy variation with lateral tip position also explains the sharp edges of the rings. In the present case, widths down to about 10 nm were observed, as shown in Fig. 1(c), which mainly depend on the spectral linewidth of the optical transition.^{5,6}

In the following, the influence of the Stark effect on the

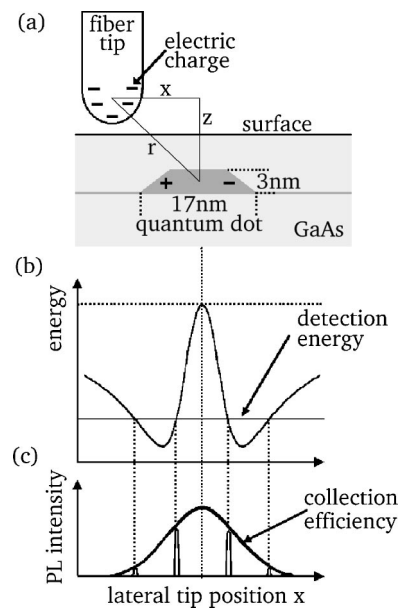


FIG. 3. (a) Schematic model for the origin of the Stark effect due to a charged fiber tip. (b) Variation of the PL energy of the quantum dot with tip position, and (c) the influence of the collection efficiency on the resulting emission features.

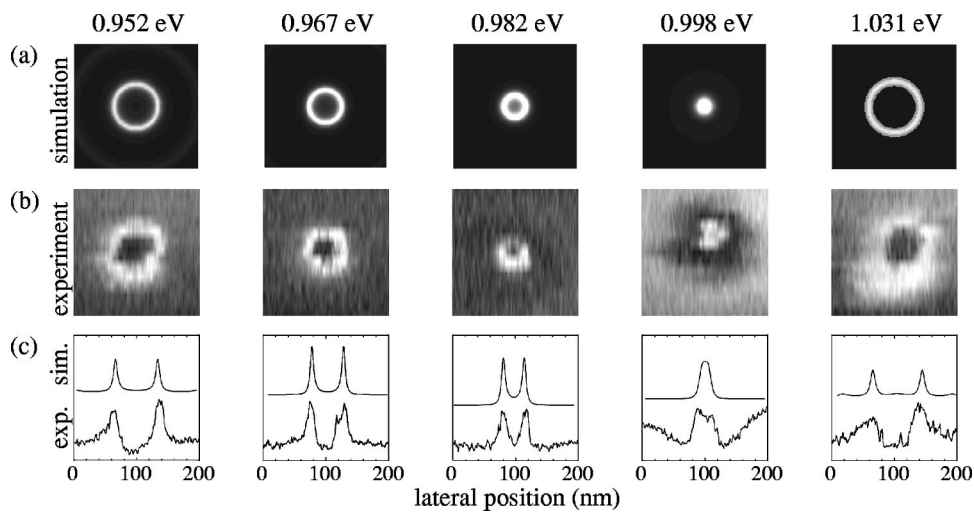


FIG. 4. Comparison of (a) simulated SNOM images with (b) the experimental data for different detection energies and (c) corresponding intensity profiles. A tip-charge-induced Stark effect was assumed for the simulations.

SNOM images is simulated quantitatively, as shown in Fig. 4. For this simulation, a parabolic potential is assumed for the electron and hole states in the quantum dot, leading to a quadratic Stark effect in the x - y direction,^{24,25} while the Stark effect in the z direction may be neglected because of the small dot height. Two transition energies at 1.00 eV and 1.09 eV with Lorentzian widths of 20 meV (Refs. 5 and 6) were assumed for the quantum-dot emission, corresponding to the first and second excited-state transitions, respectively. The ground-state transition, in contrast, is expected to be strongly suppressed due to the field-induced reduction of the overlap of electron and hole wave functions.

For determining the signal intensity, the excitation radiation of the tip is assumed to vary with $1/r^2$. For the detection an arbitrary in-plane polarization of the quantum-dot emission is used.^{26,27} This radiation is collected by the tip using the collection efficiency of a near-field dipole polarized in the x - y direction.²⁸

A good agreement with the experimental data was obtained by approximating the charged tip by a point charge of about 400 e in the center of the spherical tip apex with a radius of 60 nm, leading to a maximum x - y component of the electric field of about 300 kV/cm. It should be noted that the dielectric properties of tip and sample only result in a screening of the electric field, so that they could be neglected here for simplicity. A more sophisticated treatment considering dielectric effects and the true tip geometry only would yield a larger tip charge with otherwise very similar simulation parameters.

The results of the simulation in comparison with the respective experimental images are presented in Fig. 4 for different detection energies. An excellent agreement of the simulation with the data is found. Both the diameters of the rings and their disappearance are described by the model. Only the depressions observed experimentally at 0.952 eV and 0.998 eV within the rings are not found in the simulations. This effect is not understood up to now and requires further investigation.

Finally it should be noticed that it is irrelevant for this model if the fiber tip is charged itself or if charges develop at or underneath the sample surface. In both cases no ground connection is provided, which could be realized, e.g., by a metal coating of the tip.

In conclusion, we observed ringlike emission features in SNOM images of single InGaAs quantum dots. Because of the observed strong variation of the ring diameter with the detection energy, a tip-charge induced Stark shift of the emission lines was assumed. A simulation of the emission profiles resulted in an excellent agreement with the experimental data. Our results also demonstrate that a SNOM tip is capable to apply strong electric fields to the investigated objects. If this effect can be better controlled in the future, e.g., by biasing a metal-coated tip, an interesting new field of SNOM applications would develop.

F. Heinrichsdorff and D. Bimberg are acknowledged for providing the samples.

*Electronic address: geller@physik.tu-berlin.de

¹M. A. Paesler and P. J. Moyer, *Near-Field Optics: Theory, Instrumentation and Applications* (Wiley-Interscience, New York, 1996).

²H.F. Hess, E. Betzig, T.D. Harris, L.N. Pfeiffer, and K.W. West, *Science* **264**, 1740 (1994).

³G. Guttroff, M. Bayer, A. Forchel, D.V. Kazantsev, M.K. Zundel, and K. Eberl, *JETP Lett.* **66**, 528 (1997).

⁴V. Sandoghdar, S. Wegscheider, G. Krausch, and J. Mlynek, *J. Appl. Phys.* **81**, 2499 (1997).

⁵J.L. Spithoven, J. Lorbacher, I. Manke, F. Heinrichsdorff, A. Krost, D. Bimberg, and M. Dähne-Prietsch, *J. Vac. Sci. Technol. B* **17**, 1632 (1999).

⁶I. Manke, J. Lorbacher, J.L. Spithoven, F. Heinrichsdorff, and M. Dähne-Prietsch, *Surf. Interface Anal.* **27**, 491 (1999).

⁷D. Pahlke, I. Manke, F. Heinrichsdorff, M. Dähne-Prietsch, and W. Richter, *Appl. Surf. Sci.* **123/124**, 400 (1998).

⁸I. Manke, D. Pahlke, J. Lorbacher, W. Busse, T. Kalka, W. Richter, and M. Dähne-Prietsch, *Appl. Phys. A: Mater. Sci. Process.* **66**, 381 (1998).

- ⁹F. Heinrichsdorff, A. Krost, M. Grundmann, D. Bimberg, F. Bertram, J. Christen, A. Kosogov, and P. Werner, *J. Cryst. Growth* **170**, 568 (1997).
- ¹⁰F. Heinrichsdorff, A. Krost, M. Grundmann, D. Bimberg, A. Kosogov, P. Werner, F. Bertram, and J. Christen, in *The Physics of Semiconductors*, edited by M. Scheffler and R. Zimmermann (World Scientific, Singapore, 1996), p. 1321.
- ¹¹E. Betzig, J.K. Trautman, J.S. Werner, T.D. Harris, and R. Wolfe, *Appl. Opt.* **31**, 4563 (1992).
- ¹²E. Betzig and R.J. Chichester, *Science* **262**, 1422 (1993).
- ¹³B. Hanewinkel, A. Knorr, P. Thomas, and S.W. Koch, *Phys. Rev. B* **55**, 13 715 (1997).
- ¹⁴A. Chavez-Pirson and S.T. Chu, *Appl. Phys. Lett.* **74**, 1507 (1999).
- ¹⁵G.W. Wen, J.Y. Lin, H.X. Jiang, and Z. Chen, *Phys. Rev. B* **52**, 5913 (1995).
- ¹⁶S. Raymond, J.P. Reynolds, J.L. Merz, S. Fafard, Y. Feng, and S. Charbonneau, *Phys. Rev. B* **58**, 13 415 (1998).
- ¹⁷I.E. Itskevich, S.I. Rybchenko, I.I. Tartakovskii, S.T. Stoddart, A. Levin, P.C. Main, L. Eaves, M. Henini, and S. Parnell, *Appl. Phys. Lett.* **76**, 3932 (2000).
- ¹⁸H. Htoon, J.W. Keto, O. Baklenov, A.L. Holmes, Jr., and C.K. Shih, *Appl. Phys. Lett.* **76**, 700 (2000).
- ¹⁹A. Patanè, A. Levin, A. Polimeni, F. Schindler, P.C. Main, L. Eaves, and M. Henini, *Appl. Phys. Lett.* **77**, 2979 (2000).
- ²⁰V. Türck, S. Rodt, O. Stier, R. Heitz, R. Engelhardt, U.W. Pohl, D. Bimberg, and R. Steingrüber, *Phys. Rev. B* **61**, 9944 (2000).
- ²¹S.-S. Li and J.-B. Xia, *J. Appl. Phys.* **88**, 7171 (2000).
- ²²T.M. Hsu, W.-H. Chang, C.C. Huang, N.T. Yeh, and J.-I. Chyi, *Appl. Phys. Lett.* **78**, 1760 (2001).
- ²³H. Eisele, O. Flebbe, T. Kalka, C. Preinesberger, F. Heinrichsdorff, A. Krost, D. Bimberg, and M. Dähne-Prietsch, *Appl. Phys. Lett.* **75**, 106 (1999).
- ²⁴C. Cohen-Tannoudji, B. Diu, and F. Laloë, *Quantum Mechanics* (Wiley, New York, 1977), Vol. 1.
- ²⁵D. Bimberg, M. Grundmann, and N.N. Ledentsov, *Quantum Dot Heterostructures* (Wiley, Chichester, 1999).
- ²⁶O. Stier, M. Grundmann, and D. Bimberg, *Phys. Rev. B* **59**, 5688 (1999).
- ²⁷A.J. Williamson, L.W. Wang, and A. Zunger, *Phys. Rev. B* **62**, 12 963 (2000).
- ²⁸J.D. Jackson, *Classical Electrodynamics* (Wiley, New York, 1962).